

---

# Accurate Attenuation Correction Despite Movement during PET Imaging

Jesper L.R. Andersson, Bengt E. Vagnhammar and Harald Schneider

*Uppsala University PET Centre, Department of Radiation Sciences, Subfemtomole Biorecognition Project, Uppsala University, Uppsala, Sweden*

---

Recent methods to realign PET images are useful to correct minor changes in position due to subject movement. When using measured attenuation correction in the presence of larger subject movements, the attenuation data will not correctly represent the conditions of the emission scan and hence lead to erroneous attenuation correction. **Methods:** In the presence of subject movement between two emission scans (EM1 and EM2), the first scan was assumed to be correctly aligned with the transmission scan. The emission scans were reconstructed without attenuation correction and were realigned so that the transformation matrix mapping EM2 onto EM1 was found. The inverse of that matrix was used to reslice the transmission images. The resliced transmission images were forward projected to yield new attenuation data and EM2 was re-reconstructed. Finally, the image set from EM2 was resliced to match the orientation of EM1. The method was validated by phantom data and by human brain and cardiac studies. **Results:** Phantom data show that accurate attenuation correction can be achieved by reslicing the transmission images. In 795 region of interest measurements, the mean error after reslicing was  $-0.8\%$ , the standard deviation of the error was  $3.8\%$  and the maximum error was no greater than  $11.7\%$ . Results from human brain and cardiac experiments yield similar results with a maximum error of  $7.5\%$  in 80 measurements. **Conclusion:** Reslicing of attenuation data with transformation parameters obtained from realignment of emission data provides an accurate and reliable method to obtain correct quantification in the presence of changes in position due to subject movement during or between PET examinations.

**Key Words:** positron emission tomography; attenuation correction; image registration

**J Nucl Med 1995; 36:670-678**

---

**T**he emergence of methods to retrospectively realign PET scans (1-7) is an important step towards solving the problem of patient movement during or between PET examinations. These methods all use one dataset as a point of reference that is held stationary and proceed by realigning one or several other scans to match the reference. They

can be used to correct movements between examinations to allow, for example, subtraction between subsequent examinations. They may also be used to correct movements between individual frames in a dynamic study prior to further analysis. The accompanying problem of performing an adequate attenuation correction has achieved less attention. In a typical setting one transmission scan is performed, followed by several emission scans after one or more injections of tracer. Even when there are several injections of tracer, the transmission scan is rarely repeated. Thus, if there are movements between the emission scans, there will also have been movements relative to the transmission scan. Effects of misalignment between true and assumed attenuating media are well known (8) and misalignment between transmission and emission scans has been shown to have a large impact on quantification in cardiac studies (9). A possible remedy for this problem in brain studies would be the use of calculated attenuation correction (10,11) evaluated separately for each emission dataset. The weak points of those methods are the need for a relatively high uptake in superficial soft tissue, adequate counting statistics and their exclusion from the chest region. The use of a transmission scan to perform attenuation correction has important advantages. It gives accurate values in the presence of air, lung or bone and is applicable to data obtained with any type of tracer regardless of uptake in superficial tissue. Noise propagation from the transmission scan into the emission scan can be addressed by segmentation methods (12-14). Recently, a method was suggested to realign transmission scans to each other (4,15), to allow for reuse of high count transmission scans by alignment to subsequent short transmission scans. It was also suggested for use in alignment of emission scans by assuming lack of movement between a transmission scan and its appurtenant emission scan (4).

In this article, we present the implementation and validation of a method that attempts to solve the problem of attaining proper attenuation correction in the presence of position changes due to subject movement between the emission scanning sessions. The method is validated on phantom data, and on human brain and cardiac data. The effect of mismatch between transmission and emission scans for brain studies is also investigated.

---

Received Apr. 13, 1994; revision accepted Sept. 20, 1994.  
For correspondence or reprints contact: Jesper Andersson, MSc, Uppsala University PET Centre, S-751 85 Uppsala, Sweden.

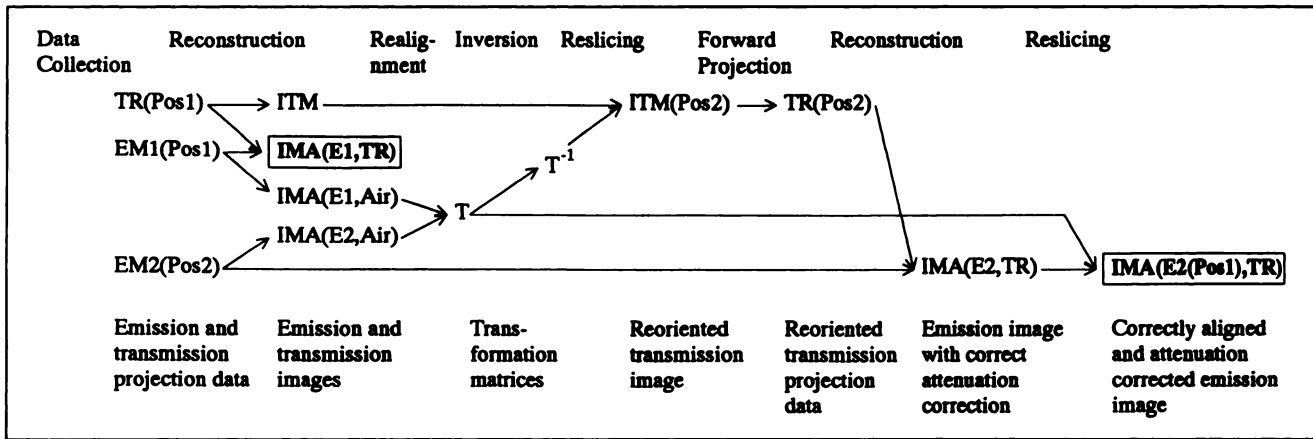


**FIGURE 1.** (Top) Operation being performed. (Middle) Output from the operation. (Bottom) Format of the output. The output from the whole procedure is marked by boxes and consists of the following data: IMA(E1,TR): emission image obtained before movement reconstructed with the original attenuation scan; and IMA(E2(pos1),TR): emission image obtained after movement, reconstructed with realigned attenuation scan and resliced to match the orientation of IMA(E1,TR). EM = emission projection data; TR = transmission projection data; IMA = emission image data; ITM = transmission image data; IMA(E1,TR) = emission image data obtained by reconstructing EM1 using TR for attenuation correction; IMA(E#,Air) = emission image data obtained by reconstructing E# without attenuation correction; T = transformation matrix mapping IMA(E2,Air) onto IMA(E1,Air).

## METHODS

### Theory

Attenuation measurement in PET is performed by doing two measurements with an external positron-emitting source in the scanner, one with and one without the object, for which the attenuation is sought. The ratio between these two measurements is then used to correct the data from the emission scan. An image of the attenuating object can be generated by reconstruction of the logarithm of the ratio projections. By doing forward projection through the full volume of transmission images, it is possible to deduce the attenuation along a ray in any direction through the volume. Thus, by reorienting the volume and forward projecting the resulting images, attenuation data can be evaluated as if the object had been oriented differently at the time of scanning. The negative consequences will be data loss in the axial direction.

A method to realign PET emission scans that is rapid and robust enough to permit its use on individual frames in dynamic studies has been developed at our facility (7). It uses one emission dataset as the reference and realigns one or several other emission datasets to that reference. High speed and accuracy is achieved by using image edge information obtained by differentiation of the images. Image volumes are resliced using trilinear interpolation.

Consider the case where one transmission scan (TR) and two emission scans (EM1 and EM2) have been obtained, and where there has been a change in position between the two emission scans. It is assumed that the TR is correctly aligned to the EM1. The matrix found by the realignment program to map the EM2 to EM1 is inverted and applied to TR. This will reorient TR so that it matches the position of EM2. The reoriented transmission dataset is forward projected so that attenuation correction data are created for EM2. EM2 is then reconstructed again from its projection data, now with the reoriented attenuation correction data. Finally, the re-reconstructed EM2 is reoriented using the original transfer matrix to match the position of EM1. The full procedure of the method is demonstrated graphically in Figure 1.

The method involves stepping back and forth between the projection space and the image space. This is time-consuming but necessary, since the realignment must be done in the image space.

Realignment of PET data is a three-dimensional problem with six degrees of freedom, three translations and three rotations. If direct realignment is attempted in the projection space, only the inplane translations and rotation will be available.

Out-of-plane rotations and translations of transmission volume will result in full or partial data loss in the extreme slices. Those slices can not be forward projected and they will not be reconstructed in the re-reconstruction of EM2.

### PET Scans

**Scanners.** Phantom studies and brain studies were performed on a GEMS 2048-15B scanner (16) and cardiac studies on a GEMS 4096-15WB (17). Both scanners produce 15 slices with 6.5-mm slice spacing and have a 6-mm axial and transaxial FWHM.

**Phantom Studies.** A plastic phantom with an outer diameter of 205 mm and inner diameter of 195 mm containing five air-filled glass spheres of diameters 15, 22, 27, 34 and 40 mm was filled with water, positioned in the gantry and a 2-min transmission scan was obtained using a rotating 140 MBq  $^{68}\text{Ge}$  pin source. The phantom was translated 5, 10 and 15 mm upward in the gantry and 5, 10 and 15 mm toward the back of the scanner in the axial direction; the scanner gantry was tilted 5 and 10 degrees counterclockwise around the x-axis. Transmission scans were obtained in all nine positions. The phantom was removed from the scanner, 100 MBq of  $^{18}\text{F}$ -FDG were injected and the phantom was carefully repositioned in the scanner. Four-minute emission scans were obtained in all the positions for which transmission scans had been made. The accuracy of repositioning was estimated to be  $\pm 1$  mm.

**Brain Studies.** An unconscious and respirator-ventilated subject was positioned in the scanner. A 10-min transmission scan was obtained using a rotating 52 MBq  $^{68}\text{Ge}$  pin source. An injection of 1000 MBq of  $^{15}\text{O}$ -water was made and a dynamic scan sequence consisting of seventeen 5-sec frames and two 20-sec frames was started. All individual frames and a summation frame consisting of all frames were reconstructed with an 8-mm Hanning filter, 2 mm pixel size, using the transmission scan for attenuation correction. Eight days later, the same protocol was repeated.

**Cardiac Studies.** An otherwise healthy subject with previously suspected myocarditis was positioned in the scanner with his arms

extended behind his head. A 10-min transmission scan was obtained using a rotating 140 MBq  $^{68}\text{Ge}$  pin source. Carbon-11-acetate (570 MBq) was injected and a dynamic scan sequence consisting of ten 6-sec frames, four 1-min frames, five 2-min frames, five 3-min frames and four 5-min frames was started. All individual frames and a summation frame, consisting of four 1-min frames starting 2 min after injection, were reconstructed with a 6-mm Hanning filter, 4 mm pixel size, using the transmission scan for attenuation correction. The subject was removed from the scanner and 3 hr were allowed for tracer decay. The subject was repositioned in the scanner while exercising on an electrically braked bicycle ergometer. A transmission and an emission study were performed with a shortened version of the above protocol, but 1130 MBq  $^{11}\text{C}$ -acetate were injected.

### Verification Methods

*Verification of Forward Projection.* For one human brain study, transmission images and emission images were reconstructed using measured attenuation correction. The transmission images were forward projected, generating a new set of attenuation correction data, and new emission images were reconstructed using the forward projected data from attenuation correction. The two sets of emission images were compared visually and by visual inspection of images generated by dividing one of the sets by the other. Furthermore, a scatter plot with the pixel value of the original dataset on the x-axis and the pixel value of the other dataset on the y-axis was created for 2000 pixels randomly selected from within the brain contour.

*Effect of Transmission-Emission Mismatch for Brain Studies.* Emission images were reconstructed for one human brain study using measured attenuation correction. Transmission images were reconstructed and 15 translated transmission image sets were created by software translation of the original transmission volume of 5, 10 and 15 mm positively and negatively in the x- and y-directions and positively in the z-direction. Transmission datasets were created by forward projection of the translated volumes, and 15 additional emission image sets were created by reconstructing the original emission data using the translated transmission datasets. Regions of interest (ROIs) of 1 cm thickness were defined in the frontal, posterior and lateral regions and in the superior cortex. Mean values of activity within the ROIs were measured in all 16 image sets.

*Verification of Accuracy of Attenuation Data Realigned Using the Emission Images.* The method outlined in Figure 1 produces as output a presumably accurate attenuation corrected image (IMA(E2(pos1),TR)). To verify the method, another transmission scan, obtained in position 2, is needed. By reconstructing EM2 with the transmission scan used for attenuation correction, an image is generated that can verify the accuracy of IMA(E2(pos1),TR)). Since the addition of another transmission scan makes the layout symmetrical, there will be two sets of correct images, two sets of images generated with a mismatched attenuation scan and two sets of images generated with a resliced attenuation scan. A flow scheme for the verification method is outlined in Figure 2. By adding additional pairs of matched emission-transmission scans and doing all possible combinations, the number of comparisons grows rapidly.

*Verification of Accuracy of Realigned Attenuation Data for Phantom Study.* Emission and transmission scans were performed on the phantom in nine different positions, yielding a total of 18 datasets. For each emission dataset there was one transmis-

sion dataset obtained in the same position, and there were eight obtained in different mismatched positions. All emission datasets were reconstructed using all transmission datasets yielding nine accurate attenuation corrected image sets and 72 with mismatched attenuation scans. A set of translation parameters was found between all emission image sets reconstructed without attenuation correction, yielding a total of 81 translation matrices. The inverse of these translation matrices was used to reslice the attenuation scans. The resliced attenuation scans were forward projected to yield new sets of attenuation data to re-reconstruct the emission images. Figure 2 depicts the design described above for the case where there are two emission and two transmission scans. The correctly reconstructed images were compared visually to the images reconstructed with misaligned transmission data and to the images reconstructed with the resliced transmission data. To obtain numerical data, 12 ROIs were drawn in each correctly reconstructed emission image set. The ROIs were drawn near edges of the phantom and edges between air and water in the images so that a mismatch between emission and transmission should have a large effect (see Fig. 5A for examples of used ROIs). Mean activity values in the ROIs were measured in the correctly reconstructed images, in the images reconstructed with a mismatched transmission scan and in the images reconstructed with a resliced transmission scan, yielding a total of 1836 ROI values.

*Verification of Accuracy of Realigned Attenuation Data for Human Studies.* For each individual there were two transmission scans and two dynamic emission scan series. The transmission and emission scans were assumed to be correctly aligned in pairs, thus the design was identical to that shown in Figure 2. Emission scans were reconstructed with and without attenuation correction, using both the appurtenant transmission scan and the transmission scan from the other examination; emission datasets were realigned and the inverses of their transformation matrices were used to reslice the transmission datasets which were then forward projected and used to re-reconstruct the emission datasets. All obtained images were visually compared and ROIs were defined. For brain and cardiac studies, the above protocol was applied to summed emission data and to one individual frame from each emission dataset. The application to summed data mimics the situation in which there are two injections of activity for one transmission study, as is the case in activation studies and in myocardial perfusion reserve studies. The single frame case attempts to mimic the situation in which there is one transmission scan and one injection and there is subject movement during the dynamic scan sequences.

## RESULTS

*Verification of Forward Projection.* Results from a comparison between an image set reconstructed with measured attenuation correction and reconstructed with data obtained by forward projection of the attenuation images are shown in Figure 3. There was a slight underestimation of the attenuation values, and thus the activity values, when forward projecting the attenuation images. The size of the underestimation of the activity values is approximately 0.5%. Visual inspection of the emission images and of the image obtained when dividing the two emission images by each other revealed no regional changes.

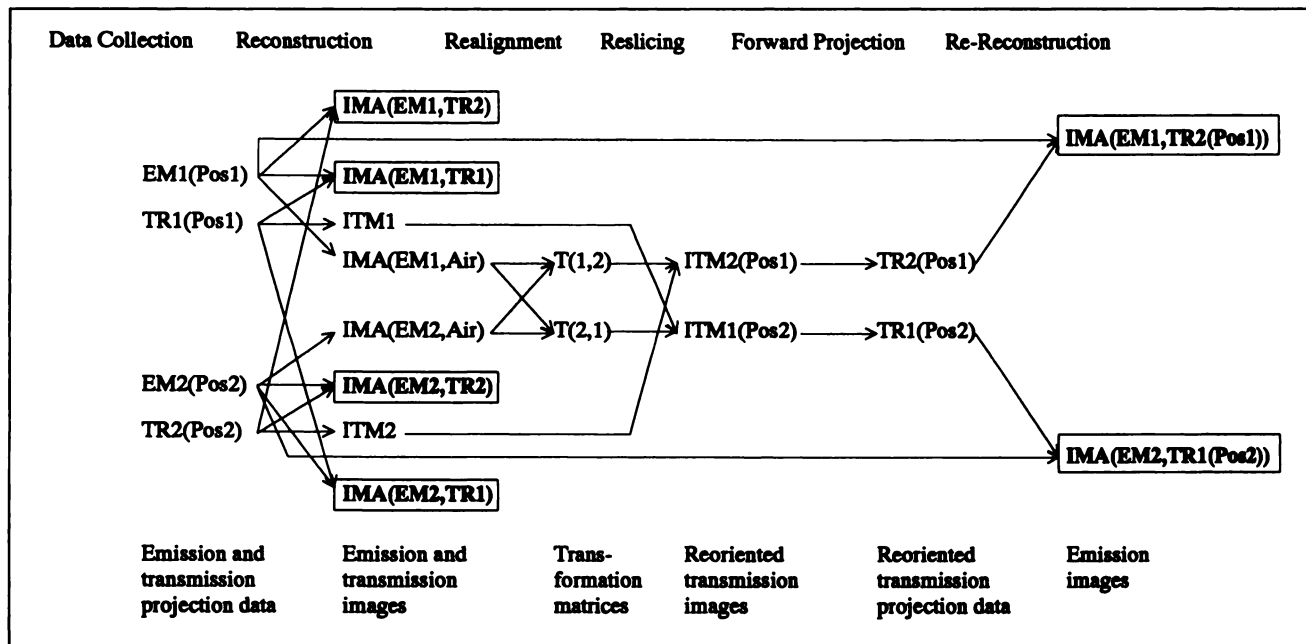


**FIGURE 2.** (Top) Operation being performed. (Middle) Output from the operation. (Bottom) Format of the output. The output from the whole procedure is marked by boxes and consists of the following data: IMA(EM1,TR1) and IMA(EM2,TR2): emission images achieved when reconstructing emission data with transmission data obtained in the same position; IMA(EM1,TR2) and IMA(EM2,TR1): emission images achieved when reconstructing emission data with transmission data achieved in the other position; and IMA(EM1,TR2(Pos1)) and IMA(EM2,TR1(Pos2)): emission images achieved when reconstructing emission data with transmission data obtained in another position, resliced to match the position of the emission data. The method is verified by comparing IMA(EM1,TR2(Pos1)) and IMA(EM2,TR1(Pos2)) with the correct images IMA(EM1,TR1) and IMA(EM2,TR2). See Figure 1 for definitions.

*Examination of the Effect of Transmission-Emission Mismatch for Brain Studies.* The ROI values obtained in the images with mismatched attenuation data compared to the values in the images with matched data are shown in Figure 4. Note how a mismatch no greater than 5 mm can produce a 10% error in a 1-cm thick cortical ROI. Data for mismatch in the z-direction are not shown.

*Verification of Accuracy of Realigned Attenuation Data for Phantom Study.* An example of a phantom study reconstructed with its matched attenuation scan (A), a mismatched attenuation scan (B) and a resliced attenuation scan (C) is shown in Figure 5. Note how the erroneous distribution of activity in the y-direction in panel B disappears in panel C. Note also how the holes in the phantom seem to have moved upwards in panel B compared to in panel A. The reason for this is that the effect from the hole in the attenuation data is larger than the effect from the hole in the emission data. When reconstructing the same phantom without attenuation correction, the holes actually appear as weak hot spots.

ROI values for one of the emission datasets reconstructed with matched and mismatched attenuation data are shown in Figure 6. An estimate of the errors can be obtained by comparing a ROI value obtained in an emission image reconstructed with its appurtenant transmission scan to a ROI value obtained in the same emission data reconstructed with another transmission scan. By doing this for all possible ROIs across all phantom data, before

and after reslicing of the attenuation data, a good statistical estimate was achieved for the errors associated with the method. These data are presented in Table 1 and Figure 7. A normal probability plot of the errors after alignment of

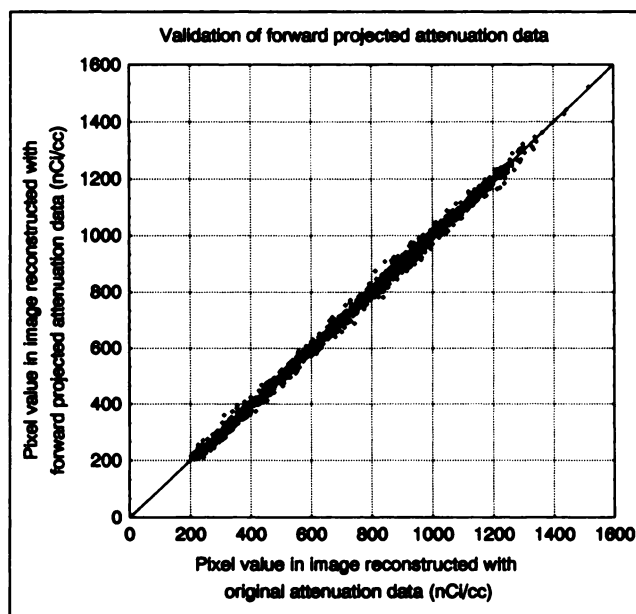


**FIGURE 3.** Scatter plot compares emission image reconstructed with original attenuation data to an emission reconstructed with attenuation data obtained by forward projection of transmission images.

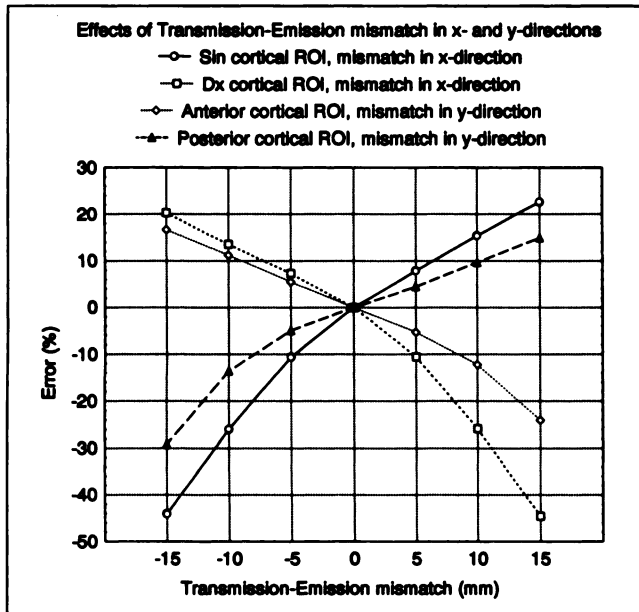


**FIGURE 4.** Plot shows the effect of a mismatch between emission and transmission data for a brain study.

transmission data shows excellent agreement with a normal distribution. Since not all slices were possible to reconstruct after reslicing of the transmission data, values were not obtained for all ROIs after the second reconstruction. Those ROI values were also excluded from analysis in the pre-reslicing images. Thus, a total of 795 ROI values were obtained before and after reslicing of the transmission data.

**Verification of Accuracy of Realigned Attenuation Data for Human Studies.** Examples of images reconstructed with its original transmission dataset (D and G), with a mismatched transmission dataset (E and H) and with a mismatched transmission dataset resliced to match the emission data (F and I) are shown in Figure 5 for the brain and cardiac studies, respectively. Note how the activity distribution changes drastically when images are reconstructed with mismatched attenuation data (Fig. 5E and H). In the cardiac case, data would actually indicate a substantial hypoperfusion in the lateral chamber wall, and might mislead the diagnosis. After reslicing of transmission data (Fig. 5F and I) the emission images look very similar to those obtained with the original transmission data. ROI values for both emission datasets, both single frames and summed data are presented in Table 2 and Figures 8 and 9. The maximum errors for the brain and cardiac studies are 7.5% and 6.5%, respectively.

## DISCUSSION

We have shown that our method is capable of attaining accurate attenuation correction despite subject movement between scan sessions, provided there was no change in position between the transmission and the first emission scan. A complicated PET protocol with multiple injections with the same or different tracers may last for more than an

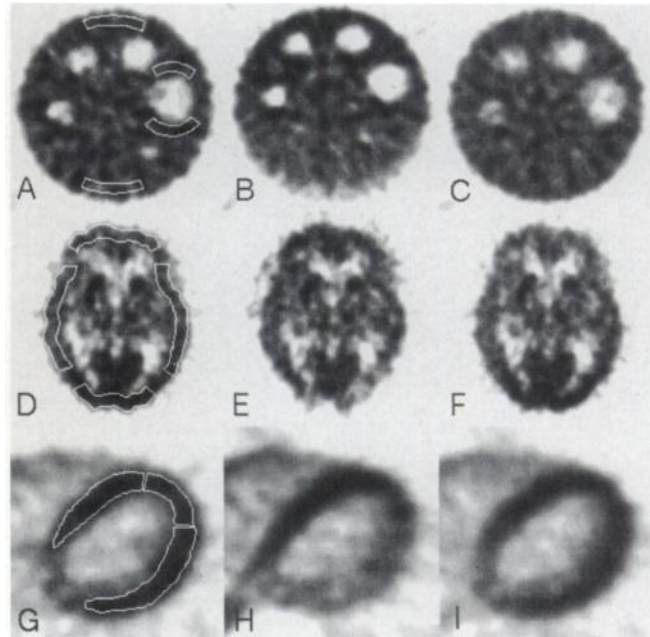


**FIGURE 5.** Results from phantom, brain and cardiac experiments. (A) Phantom image reconstructed with matched attenuation scan. (B) The same emission dataset as in (A), reconstructed with an attenuation scan translated 15 mm in the y-direction compared to the emission scan. Note how the holes from the air cavities have moved and follow the transmission rather than the emission data. (C) The same emission dataset reconstructed with an attenuation scan translated 15 mm in the y-direction compared to the emission scan after reslicing of attenuation scan with the transformation matrix obtained when realigning emission images to each other. (D) Brain image reconstructed with matched attenuation scan. (E) The same emission dataset as in (D), reconstructed with a mismatched attenuation scan. (F) The same emission dataset as in (D), reconstructed with the mismatched attenuation scan after reslicing with the transformation matrix obtained when realigning emission images to each other. (G) Cardiac image reconstructed with matched attenuation scan. (H) The same emission dataset as in (G), reconstructed with a mismatched attenuation scan. (I) The same emission dataset as in (G), reconstructed with the mismatched attenuation scan after reslicing with the transformation matrix obtained when realigning emission images to each other.

hour, during which the subject is supposed to be motionless. During that time, however, there will have been one, or several movements that passed unnoticed, thus invalidating data after the movement. Application of this method would then correct the data and enable their use. The use of this method to obtain accurate attenuation correction does not necessitate the use of our method (7) to register emission images; indeed it could be used together with any of the published methods (1-6).

The reason for the slight underestimation of the attenuation data and the subsequent activity values in emission images during forward projection of transmission images is unclear. A possible explanation may be differences in the implementation of backprojection in the reconstruction program and implementation of forward projection in the software written during the preparation of this article. However, the small magnitude of the underestimation together with its spatial invariance makes it negligible.

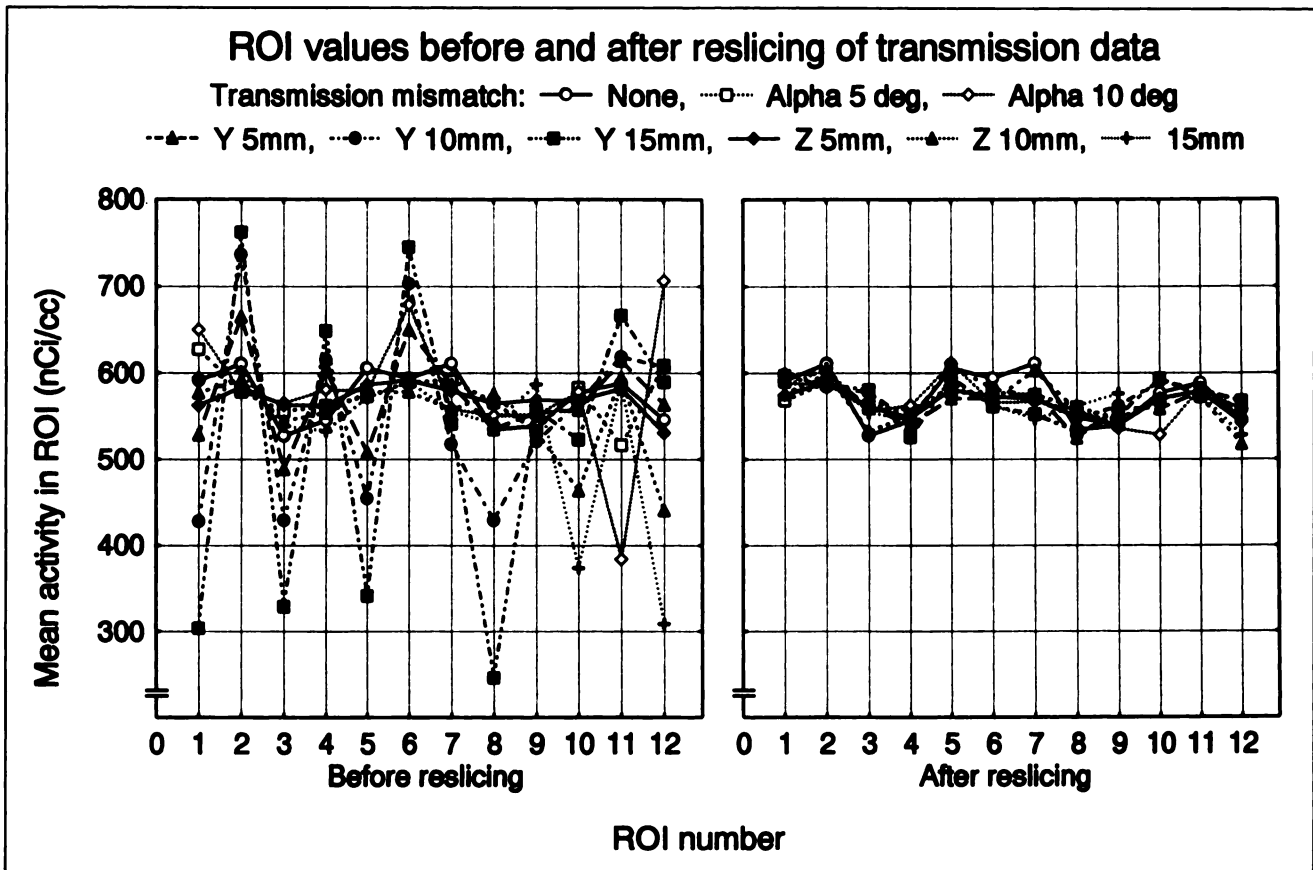


**FIGURE 6.** One phantom emission dataset reconstructed with transmission data obtained in the same position and with eight other transmission scans obtained in other positions before (left graph) and after (right graph) reslicing of attenuation data. Every point represents the mean activity within an ROI projected onto an emission image.

The effects of a mismatch between attenuation and emission scans have been shown to be severe for heart studies (8). Our data indicate that the effects are no less for brain studies, and it can be seen in Figure 4 that a mismatch of 15 mm may induce regional errors in the magnitude of 40%. Clearly, it would not be meaningful to realign an examination with movements in that magnitude if the problem of attenuation correction was not addressed at the same time. The acceptable level of quantification error, and thus subject movement, would have to be settled from case to case, but clearly 5 mm in any direction would be the upper limit for most applications.

The phantom data demonstrate the feasibility of the

method. Error distribution after realignment fits a normal distribution very well and may therefore be ascribed mainly to counting statistics. A tendency towards deteriorated

**TABLE 1**  
 Percentage Errors\* in ROI Values in Images Reconstructed with Original Matched Attenuation Data Compared to Images Reconstructed with Mismatched Attenuation Data

Reslicing	n	Before and after reslicing			s.d.
		mean	min.	max.	
Before	795	-2.68	-76.1	71.4	18.31
After	795	-0.83	-11.7	10.4	3.76

\*Errors were defined as 100 (mismatched-matched)/matched.

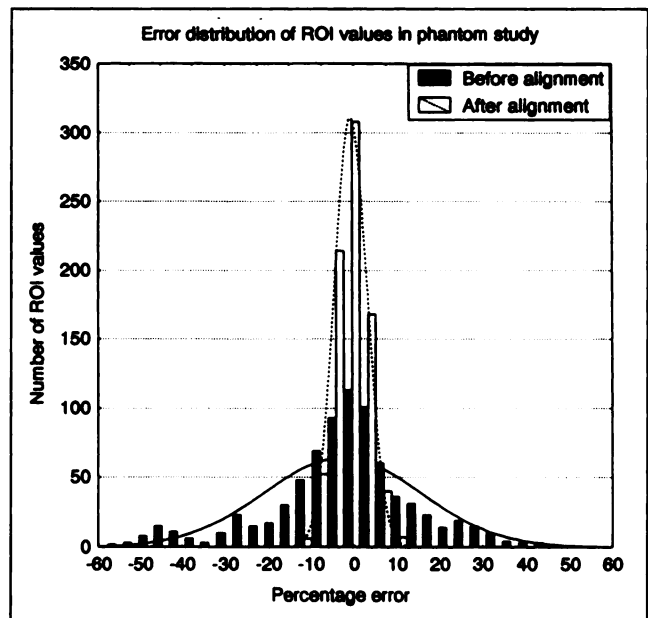


**FIGURE 7.** Registration error versus total number of counts per 15 slices. Translations and rotations in all directions are lumped and the curves represent a mean of all directions.

**TABLE 2**  
**Percentage Errors\* in ROI Values in Images Reconstructed with Resliced Attenuation Data and Images Reconstructed with Original Matched Attenuation Data**

Study	n	mean	min	max	s.d.
Brain	36	-0.68	-7.51	5.37	3.16
Heart	44	0.06	-6.06	6.46	3.54

\*Errors were defined as  $100 \times (\text{resliced-original})/\text{original}$ .

resolution near sharp edges in the phantom images was observed. This may be explained by reslicing of the transmission images which results in smoothing. This smoothing is propagated into the emission images, but will have an appreciable effect only in the areas where there are edges in the transmission images. The same effect was noticed by Bacharach et al. (4) and has been investigated by Meikle et al. (14). It influences mainly cardiac studies, where the activity in the lateral wall of the left chamber will be underestimated by no more than 5%. This effect could be avoided if the reslicing of the transmission data was com-

ined with a segmentation method (12,13). Segmentation of the transmission images after reslicing and prior to forward projection would restore the high frequencies in the images and counteract the smoothing introduced image reslicing.

Data obtained from human studies further indicate that our method produces correct results. The images reconstructed with resliced attenuation data are virtually identical to those reconstructed with the appurtenant attenuation data. Results obtained when realigning one individual frame to another are very similar to those from realigned summed data. This indicates that the method can be used for realignment and correction within a single dynamic examination as well as between examinations.

This method is similar in practice but different in essence to the method suggested by Bacharach (4) and Bettinardi (15). Their method assumes the existence of a matched transmission scan for each emission scan, and then attempts to realign examinations and/or reuse low noise attenuation data. Thus, a prerequisite is that all movements are immediately noticed, and a new transmission scan is obtained in that position before the next movement occurs. This method, on the other hand, is meant to be used ret-

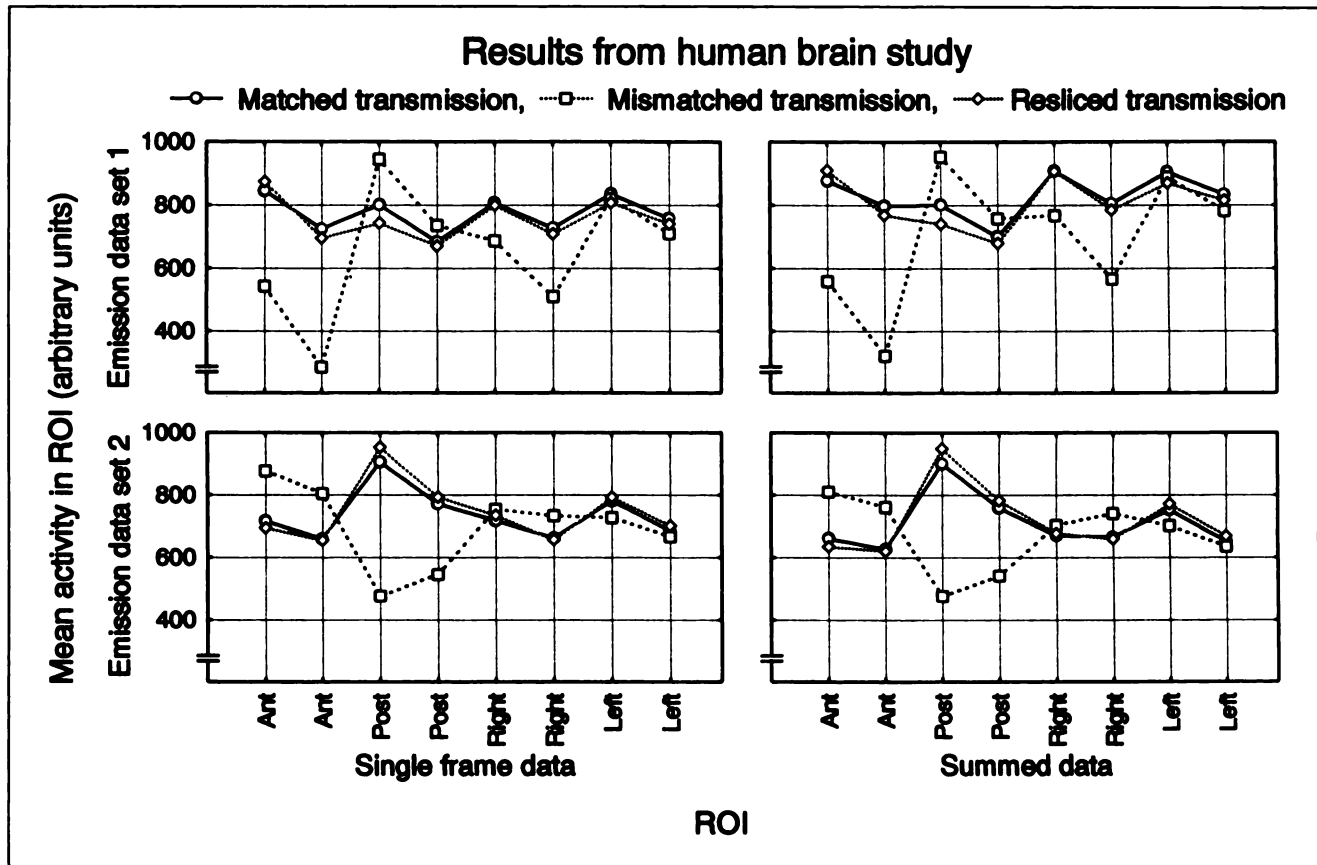


**FIGURE 8.** Results from a brain study. Comparison between ROI values obtained in the emission dataset when reconstructed with its appurtenant transmission data, with mismatched transmission data and mismatched attenuation scan after reslicing with the transformation matrix obtained from realigning emission images to each other. Every point represents a ROI value obtained in an emission image. Upper left: Single frame from brain emission dataset 1. Lower left: Single frame from brain emission dataset 2. Upper right: Summed data from brain emission dataset 1. Lower right: Summed data from brain emission dataset 2.

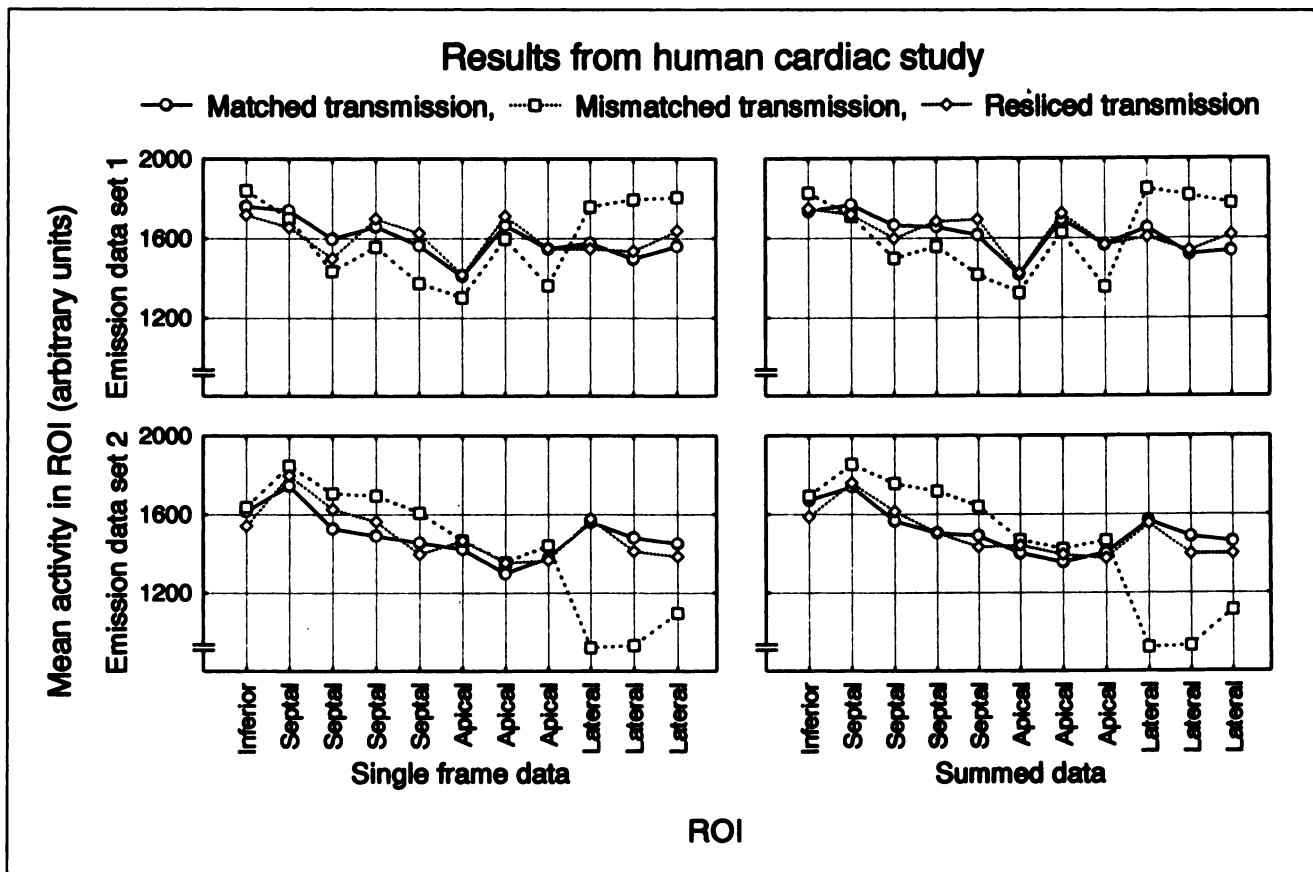


**FIGURE 9.** Results from a cardiac experiment. Comparison between ROI values obtained from the emission dataset when reconstructed with its appurtenant transmission data, with mismatched transmission data and with the mismatched attenuation scan after reslicing with the transformation matrix obtained when realigning emission images to each other. Every point represents an ROI value obtained in an emission image. Upper left: Single frame from cardiac emission dataset 1. Lower left: Single frame from cardiac emission dataset 2. Upper right: Summed data from cardiac emission dataset 1. Lower right: Summed data from cardiac emission dataset 2.

respectively in the cases where a movement is detected after completion of the examination.

A typical scenario is when movements are detected during evaluation of data from an examination in some form or another. The movements are analyzed by applying emission image realignment software to all frames in the examination by utilizing the previous of two consecutive frames as a reference. Thus, in a time series of ten frames, the first one is used as reference for the second, the resliced second is used as reference for the third, and so on. If movements exceeding 5 mm or 5° are detected, the time series is re-reconstructed without attenuation correction and is again passed to the image realignment software. The resulting nine transformation matrices are inverted and applied to the transmission images, yielding nine new sets of attenuation data. Frames 2 to 10 are finally resliced using their original transformation matrices. The result is an accurate, attenuation corrected, aligned image.

The reason for using a variable reference, and not just letting the first frame be the reference and aligning the subsequent frames to it, is that activity distribution changes during the course of the examination. It may not be possible to realign an early image showing mainly vas-

cular distribution to a late image showing mainly bound tracer.

We reconstructed the images without attenuation correction prior to realignment because our data indicate that realignment accuracy may be affected if one of the emission images contains artifacts due to a mismatched attenuation scan. In reports on realignment of PET emission data claiming submillimeter accuracy, none of the experiments were designed to examine that aspect. Whether phantom (2,5) or human (3) data were used to verify realignment, they all had accurate attenuation correction, something that clearly is not realistic if measured attenuation correction is used. The above example describes the application to a single injection, dynamic PET study, but the same strategy is applicable to activation studies or rest-stress cardiac studies.

Our method is based on the assumption that the first emission scan is correctly aligned to the transmission scan. The assumption is reasonable and will be fulfilled in most cases because the less time between transmission and emission scans, the smaller the risk for movement. There will be instances where this approach will not work, but cases where this problem occurs whenever measured at-

tenuation correction is used is not unique to this method. Activation studies are less affected since this method at least ensures that any mismatch between the transmission and the first emission scan will remain constant throughout all emission scans. This means that both baseline and activated states will be equally affected, and that the percent change between the states will not be affected at all.

A drawback of the method is data loss in the extreme slices in the event of out-of-plane translations and/or rotations. This can be avoided if two partially overlapping transmission scans, with an axial translation in between, are performed before the start of emission scanning. The emission scan would then be centered in the middle of the two transmission scans in the axial direction. Thus, movement during the emission scan with a magnitude less than half the translation between the two transmission scans would not lead to any loss of data.

An alternative method would be the use of calculated attenuation correction (10,11). We examined the method suggested by Bergström et al. (10) and found that it performs poorly in the presence of noise, as is the case when applying it individually to every frame in a dynamic protocol. The effect might be that different contours are found in different frames, aggravating rather than alleviating the problem. We have not studied the method by Siegel et al. (11) and do not know if the same is true for their approach. A common problem for both methods is that they are not applicable to the chest region.

With the expansion of clinical PET, there is a need for rapid procedures that can be tolerated by the patients. The elaborate, and uncomfortable, fixation devices traditionally used in PET cannot be applied to all categories of patients without problems. Their use may also cause unwanted effects in activation studies, where itching or pain from the fixation may alter the activation pattern. The method described above provides a way to retrospectively correct all adverse effects caused by subject movement. Performance of the full correction procedure would take approximately 5 min per frame on a VAX-station 4000/60, and a 10-frame dynamic study would thus require about 1 hr. This may seem long, but computer time should not be compared to scanner time since the cost for the two differs immensely. Furthermore, the procedure can be fully automated and would not require operator input once the program is started.

## CONCLUSION

When retrospectively realigning PET emission images, the effect of the mismatch on the attenuation correction

must be considered. When translations are larger than 5 mm the effects on quantification may be 10% or more. The method presented in this paper provides a way to correct for these effects, enabling examinations containing relatively large movements to be correctly quantified and realigned.

## ACKNOWLEDGMENTS

The authors thank Mats Bergström for his valuable advice regarding methods and experiments and Lennart Thurfjell for his kind assistance in producing the illustrations for this article.

## REFERENCES

1. Mintun MA, Lee KS. Mathematical realignment of paired PET images to enable pixel-by-pixel subtraction. *J Nucl Med* 1990;31:816.
2. Woods RP, Cherry SR, Mazziotta JC. Rapid automated algorithm for aligning and reslicing PET images. *J Comput Assist Tomogr* 1992;16:620-633.
3. Hoh CK, Dahlbom M, Harris G, et al. Automated iterative three-dimensional registration of positron emission tomography images. *J Nucl Med* 1993;34:2009-2018.
4. Bacharach SL, Douglas MA, Carson RE, et al. Three-dimensional registration of cardiac positron emission tomography attenuation scans. *J Nucl Med* 1993;34:311-321.
5. Eberl S, Kanno I, Fulton RR, et al. Automatic three-dimensional spatial alignment for correcting interstudy patient motion in serial PET studies. In: Uemura K, Lassen NA, Jones T, Kanno I, eds. *Quantification of brain function, tracer kinetics and image analysis in brain PET*. Elsevier Science Publishers B.V., Amsterdam; 1993:419-426.
6. Pelizzari CA, George TYC, Spelbring DR, Weichselbaum RR, Chen CT. Accurate three-dimensional registration of CT, PET and/or MR images of the brain. *J Comput Assist Tomogr* 1989;13:20-26.
7. Andersson JLR. A rapid and accurate method to realign PET scans utilizing image edge information. *J Nucl Med* 1994;36:000-000.
8. Huang SC, Hoffman EJ, Phelps ME, Kuhl DE. Quantification in positron emission computed tomography: II. Effects of inaccurate attenuation correction. *J Comput Assist Tomogr* 1979;3:804-814.
9. McCord ME, Bacharach SL, Bonow RO, Dilsizian V, Cuocolo A, Freeman N. Misalignment between PET transmission and emission scans: its effect on myocardial imaging. *J Nucl Med* 1992;33:1209-1214.
10. Bergström M, Litton J, Eriksson L, Bohm C, Blomqvist G. Determination of object contour from projections for attenuation correction in cranial positron emission tomography. *J Comput Assist Tomogr* 1982;6:365-372.
11. Siegel S, Dahlbom M. Implementation and evaluation of a calculated attenuation correction for PET. *IEEE Trans Nucl Sci* 1992;39:1117-1121.
12. Huang SC, Carson RE, Phelps ME, Hoffman EJ, Schelbert HR, Kuhl DE. A boundary method for attenuation correction in positron computed tomography. *J Nucl Med* 1981;22:627-637.
13. Xu EZ, Mullani NA, Gould KL, Anderson WL. A segmented attenuation correction for PET. *J Nucl Med* 1991;32:161-165.
14. Meikle SR, Dahlbom M, Cherry SR. Attenuation correction using count limited transmission data in positron emission tomography. *J Nucl Med* 1993;34:143-150.
15. Bettinardi V, Gilardi MC, Lucignani G, et al. A procedure for patient repositioning and compensation for misalignment between transmission and emission data in PET heart studies. *J Nucl Med* 1993;34:137-142.
16. Holte S, Eriksson L, Dahlbom M. A preliminary evaluation of the Scanditronix PC2048-15B brain scanner. *Eur J Nucl Med* 1989;15:719-721.
17. Kops R, Herzog H, Schmid A, Holte S, Feinendegen L. Performance characteristics of an eight ring whole-body PET scanner. *J Comput Assist Tomogr* 1990;14:437-445.